

Phototriton Cross Section of Li^6 [†]

N. K. SHERMAN,*† J. E. E. BAGLIN, AND R. O. OWENS‡

Electron Accelerator Laboratory, Yale University, New Haven, Connecticut

(Received 31 October, 1967; revised manuscript received 5 January 1968)

The phototriton cross section of Li^6 has been measured between 24- and 35-MeV photon energy. This work complements an earlier experiment which established the production of the $\text{Li}^6(\gamma,t)$ reaction by giant-resonance photons and measured the cross section between 19 and 24 MeV. The phototriton cross section of Li^6 falls monotonically from 0.46 ± 0.24 mb at 19 MeV to 0.11 ± 0.06 mb at 35 MeV. The integrated (γ,t) cross section over this energy interval is 4.9 ± 2.5 MeV mb. The measured bremsstrahlung-weighted cross section is 0.18 ± 0.09 mb. Implications concerning the nuclear size are discussed.

I. INTRODUCTION

AN interesting problem in the study of photo-nuclear reactions which remained unsolved for a long time because of experimental difficulties is the question of phototriton emission by Li^6 . It was expected that giant-resonance photons would produce tritons since isospin selection rules allow the $\text{Li}^6(\gamma,t)\text{He}^3$ reaction to occur by electric-dipole absorption, which is dominant in the nuclear photoeffect. In addition, tritons could be produced in the reactions $\text{Li}^6(\gamma,pd)\text{H}^3$ and $\text{Li}^6(\gamma,2pn)\text{H}^3$. The first attempt to observe phototritons was made by Titterton and Brinkley¹ using photographic emulsions as detectors. They used 17.6-MeV γ rays from the reaction $\text{Li}^7(p,\gamma)\text{Be}^8$. The $\text{Li}^6(\gamma,t)$ threshold is at 15.791 MeV, so they had to search for back-to-back ionization tracks caused by 1.1-MeV tritons and He^3 . These tracks would be about 8 and 3 μ long, respectively, and would be difficult to detect. They found no events, and assigned an upper limit of 0.006 ± 0.004 mb to the cross section at 17.6 MeV.

Then Volkov and Kul'chitskii² carried out a search using a detector which was sensitive to tritons corresponding to γ -ray energies greater than 30 MeV. They observed some tritons. However, the giant-resonance region remained unexplored, and the motivation to explore it became greater when Bazhanov, Komar, and Kulikov³ reported a significant disagreement with the dipole sum-rule prediction of 126 MeV mb for the integrated photoparticle cross section of Li^6 . Their experiment studied the photoneutron emission, and because of the instability of Li^5 and He^5 , it was sensitive to all $E1$ allowed reactions except the $\text{Li}^6(\gamma,t)\text{He}^3$ and $\text{Li}^6(\gamma,pd)\text{H}^3$ reactions. They found that the integrated neutron yield up to 60 MeV was 53 MeV mb.

In 1964, Sherman *et al.*⁴ observed for the first time phototritons from the giant resonance of Li^6 . Soon afterwards, Berman *et al.*⁵ reported a careful measurement of the photoneutron yield up to 32 MeV using monoenergetic γ rays. They found an integrated cross section of 27.4 MeV mb up to 32 MeV. Their cross section extrapolated to 60 MeV gives a value about 11% lower than the value of Bazhanov *et al.* for the integrated cross section. The (γ,t) cross section integrated to 24 MeV⁶ when added to either (γ,n) result produced a number which still fell far below the sum-rule⁷ prediction. The maximum observed value of the cross section was about 0.5 mb. On the other hand, a measurement of the (γ,t) cross section was reported by Komar and Makhnovsky,⁸ who obtained a peak value of 8 mb at 22 MeV. Their result can perhaps be accounted for by (n,α) background, which is extremely difficult to eliminate when using nuclear emulsions as detectors. Electronic time gating of solid-state detectors, which we have used, eliminates the tritons due to slow-neutron background.

In view of the great discrepancy with the sum rule, we continued our triton measurements up to 35 MeV. The data between 19 and 24 MeV had been obtained by using a thick barrier detector for energy measurement.^{6,9} The new data between 24 and 35 MeV was obtained by range discrimination using a thin depletion layer. The new results match up with the older data without any relative normalization. The data indicate a maximum cross section lying no higher in energy than 19 MeV, in disagreement with the cross section obtained by Manuzio *et al.*¹⁰ on the basis of rather widely spaced data. The latter group, however, agrees as to the order

† Work supported by the U. S. Atomic Energy Commission.

* Supported in part by the National Research Council of Canada.

† Present address: Foster Radiation Laboratory, McGill University, Montreal, Canada.

‡ Present address: Department of Physics, The University, Glasgow, Scotland.

¹ E. W. Titterton and T. A. Brinkley, Proc. Phys. Soc. (London) **A67**, 350 (1954).

² Yu. M. Volkov and L. A. Kul'chitskii, Zh. Eksperim. i Teor. Fiz. **42**, 108 (1962) [English transl.: Soviet Phys.—JETP **15**, 108 (1962)].

³ E. B. Bazhanov, A. P. Komar, and A. V. Kulikov, Zh. Eksperim. i Teor. Fiz. **46**, 1497 (1964) [English transl.: Soviet Phys.—JETP **19**, 1014 (1964)].

⁴ N. K. Sherman, R. C. Morrison, and J. R. Stewart, Bull. Am. Phys. Soc. **10**, 541 (1965).

⁵ B. L. Berman, R. L. Bramblett, J. T. Caldwell, R. R. Harvey, and S. C. Fultz, Phys. Rev. Letters **15**, 727 (1965).

⁶ N. K. Sherman, J. R. Stewart, and R. C. Morrison, Phys. Rev. Letters **17**, 31 (1966).

⁷ M. Gell-Mann, M. Goldberger, and W. Thirring, Phys. Rev. **95**, 1612 (1954).

⁸ A. P. Komar and E. D. Makhnovsky, Dokl. Akad. Nauk SSSR **156**, 774 (1964). [English transl.: Soviet Phys.—Doklady **9**, 463 (1964)].

⁹ N. K. Sherman, J. E. Baglin, and R. O. Owens, Bull. Am. Phys. Soc. **11**, 10 (1966); **12**, 632 (1967).

¹⁰ G. Manuzio, R. Malvano, G. Ricco, and M. Sanzone, Nuovo Cimento **40**, 300 (1965).

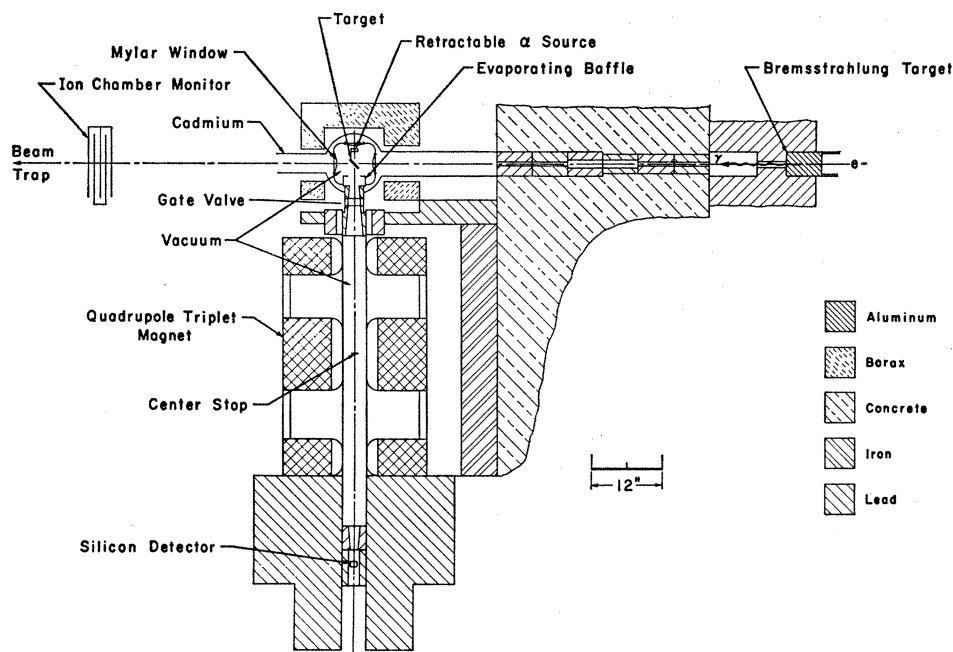


FIG. 1. Schematic diagram of the experimental layout, approximately to scale. The shielding wall around the bremsstrahlung target is shown in part only. The photon beam spends itself in a deep hole in the wall behind the ion chamber. The electron linear accelerator, not shown, is situated to the right of the figure.

of magnitude of the cross section, obtaining a maximum value of about 0.6 mb.

Denisov *et al.*¹¹ have recently reported that the maximum contribution to the (γ, t) cross section occurs between 19 and 24 MeV. They quote 12 MeV mb as the integrated phototriton cross section between 17 and 28 MeV based on the data of Makhnovsky⁸ and that of Sherman *et al.*,⁶ out of a total of 80 MeV mb for all processes up to 55 MeV. They find that above 40 MeV there is considerable 3- and 4-body production of tritons. Between 36 and 55 MeV, they find the sum of the $(\gamma, n2p)t$ and $(\gamma, pd)t$ integrated cross sections to be 5 MeV mb.

II. APPARATUS

A unique feature of the experimental arrangement which made it very useful in studying continuous-energy spectra of several charged-particle species emitted simultaneously was the ability to select an energy interval for a specific particle and adapt the detector thickness to the corresponding range of this particle. The experimental layout is shown in Fig. 1. An evaporated target, maintained in vacuum, was exposed to 40-MeV bremsstrahlung from the Yale electron linac. Charged particles emitted by the target were focused by a quadrupole triplet magnet¹² onto a Si-barrier detector. The tritons traveled entirely in vacuum between the target and the detector. The detector output was fed to a charge-sensitive preamplifier

and delay-line clipped linear amplifier. The amplified pulses were analyzed by an RIDL 400-channel pulse-height analyzer which was gated on only during the linac beam burst.

The target chamber was designed to minimize background and to permit chemically active targets to be made and maintained in vacuum. Aluminum was chosen as the chamber material. The photon beam entered and left the chamber through Mylar windows 3 in. in diam. Photoparticles passed through a vacuum gate valve through which target evaporation was also performed. Four solid targets and one gaseous target were attached, one above the other, to a movable "ladder." Gases were admitted to the gas cell via a hollow tube which served as a sliding support for the target ladder. The ladder was raised and lowered by remote control. The foil targets bisected the angle between the beam axis and the quadrupole axis, while the gas cell was axial with the beam.

An α -particle source, Am^{241} electrodeposited on platinum, was fixed on a sliding rod which entered the bottom of the vacuum chamber. The source could be raised up behind the targets, onto the quadrupole axis, for transmission measurement of target thickness.

In order to protect the detector from vacuum-pump oil the quadrupole tube was roughed down to forepump pressure and then valved off from the pump. It was then cryopumped by Zeolite contained in a trap cooled by liquid nitrogen. The Li targets remained clean during runs of a week, pumped only by the trap. Care was taken never to apply bias voltage when the pressure in the system was around 50 μ , to avoid corona damage to the detector.

¹¹ V. P. Denisov, A. P. Komar, L. A. Kul'chitskii, and E. D. Makhnovsky, *Yadern. Fiz.* 5, 498 (1967) [English transl.: *Soviet J. Nucl. Phys.* 5, 349 (1967)].

¹² J. S. O'Connell, R. C. Morrison, and J. R. Stewart, *Nucl. Instr. Methods* 30, 229 (1964).

The quadrupole triplet vacuum pipe was 4 in. in diam. The first quadrupole was chosen¹² so that it was focusing in the vertical plane and defocusing in the horizontal plane, so as to limit the band of accepted emission angles and minimize kinematic energy spread. The large-acceptance solid angle of about 0.015 sr was crucial for obtaining good statistics. The transmission function of the magnet is shown in Fig. 2.

The bremsstrahlung from the production target was collimated by lead cylinders inserted in the shielding wall as shown in Fig. 1. An ionization chamber filled with methane and argon and faced with 3 in. of Al was used to monitor the photon beam intensity. The bremsstrahlung spectral shape up to 17 MeV was obtained by measurement of the photoprotons from deuterium. The spectral shape above 17 MeV was taken to be that measured under the same conditions by Stewart and Edge¹³ using a Li-drifted Si detector capable of stopping 30-MeV protons. In Appendix A the method of calculating the photon energy corresponding to a detected triton energy is described.

The deuterium gas cell was adapted from ones used by Morrison *et al.*¹⁴ and consisted of a thin-walled brass cylinder $1\frac{1}{2}$ in. in diam and 2 in. long with two side windows, $\frac{3}{4}$ in. long by 1 in. along the arc, made of $\frac{1}{4}$ -mil Havar.¹⁵ Photoparticles emitted through one of the windows were accepted by the quadrupole magnet. The function of the other window was to keep the amount of metal seen by the magnet to a minimum to reduce background. The photon beam entered one end of the cell via a 1-in. diam hemispherical Mylar window 1 mil thick capable of withstanding 4-atm pressure.¹⁶ The beam left the cell through a brass end window 6 mil thick. Epoxy cement was used to seal the Havar and Mylar windows. Reasonable care in applying the epoxy resulted in vacuum tightness sufficient to permit the target chamber to be pumped down to 2×10^{-6} Torr for vacuum evaporation.

The Li targets were made by evaporating separated isotopes onto thin Formvar films of dimensions $1 \times 1\frac{1}{2}$ in. The films were made by dissolving Formvar in ethylene dichloride and allowing drops of the solution to fall upon the surface of distilled water. The film thickness was measured by the energy shift of monoenergetic α particles. Lithium to be evaporated was gently heated in vacuum until organic vapors were driven off. The pressure could then be brought down to 2×10^{-6} Torr. The temperature was then raised to drive surface contaminants off onto a baffle. When clean Li began to come off, the baffle was opened. Once a deposit of metal had built up on the backing, the rate of evaporation could be increased.

¹³ J. R. Stewart and R. Edge (private communication).

¹⁴ J. R. Stewart, R. C. Morrison, and J. S. O'Connell, *Phys. Rev.* **138**, B372 (1965).

¹⁵ Precision Metals Division, Hamilton Watch Company, Lancaster, Pa.

¹⁶ The Havar windows could withstand more than 6 atm.

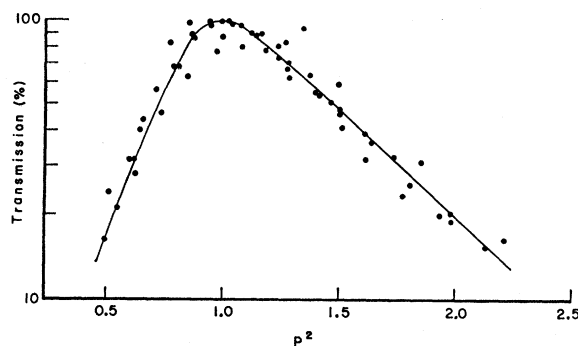


FIG. 2. Transmission function of the quadrupole triplet magnet, obtained experimentally. The percent transmission of a given charged-particle species is plotted as a function of a reduced coordinate proportional to particle energy divided by magnet current squared.

The properties of the quadrupole triplet magnet as a momentum spectrometer have been discussed by O'Connell *et al.*¹² Details relevant to this experiment have been described by Sherman *et al.*¹⁷ If the transmission peak at energy T has energy width λ at half-maximum, a criterion for resolution of particle species i from species j having different charge or mass is that

$$T_i + \lambda_i = T_j - \lambda_j. \quad (1)$$

Now

$$\lambda_i/T_i \simeq \lambda_j/T_j \equiv \lambda/T, \quad (2)$$

so that

$$(\Delta p/p)_{ij} = \frac{1}{2}(1 - T_i/T_j)/(1 + T_i/T_j). \quad (3)$$

Momentum resolution is determined by the object size (the beam-spot diameter) and the image size (the exposed diameter of the detector). The experimental resolution was 14%, corresponding to a $\frac{5}{8}$ -in. diam beam and a $\frac{3}{4}$ -in. diam detector.

The kinetic energy of the tritons focused by the quadrupole magnet was measured by means of an Ortec Si-barrier detector with a maximum depletion-layer thickness of 800μ which was attained at 300-V bias. An annular brass stop ahead of the detector reduced transmission halo but did not reduce the effective diameter. The front face of the detector was covered with a thin film of evaporated gold. The diode material was N -type silicon, whose resistivity was measured to be $9.5\text{-}k\Omega$ cm from proton cutoff energies. The energy scale was fixed by the position of the Am^{241} α line (5.477 MeV) in each spectrum. The over-all resolution obtained with α particles and a precision pulser was measured with the accelerator beam on and off. The electronics contributed 30.7 keV to the resolution, the detector contributed 86.7 keV, and pulse pileup and rf noise pickup contributed 103 keV. Under quiescent conditions, the resolution for α particles was 92.1 keV, and was 138 keV during experimental runs. The (n, α)

¹⁷ N. K. Sherman, J. E. Baglin, R. C. Morrison, R. O. Owens, J. R. Stewart, and H. L. Schultz, Yale Internal Report No. 2627-15, 1965 (unpublished).

peak obtained when the detector was ungated was 77 keV wide, indicating a total resolution of 129 keV for phototritons when pileup is folded back in. The total experimental energy resolution is discussed in Appendix B.

III. BACKGROUND SUPPRESSION

A. Slow-Neutron Background

An important feature of this experiment was the time gating of the pulse-height analyzer so that only those events occurring during the photon beam burst were recorded. This was necessary to discriminate against tritons from the $\text{Li}^6(n,\alpha)$ reaction. Thermal neutrons captured by Li^6 release tritons of 2.73 MeV, which if mistaken for phototritons give a value of k , according to Eq. (A11), in the region of 21.3 MeV, with variation from this value depending on the detection angle. (The cross section of Li^6 for thermal neutrons is about 500 b.¹⁸ If gated detectors are employed with a pulsed photon source, the (n,α) background can be greatly reduced. In this experiment the detection gate was 5 μsec long. When the pulse-height analyzer was ungated, a spike 77 keV wide at half-maximum appeared in the spectrum at 2.73 MeV (corrected for energy loss in the target). This spike was used as an energy-calibration point.

Fast-neutron contamination of the photon beam could lead to tritons of energies higher or lower than 2.73 MeV. To test this possibility, neutron filters were placed in the beam collimator. The ratio of the number of phototritons to photoprotons and the shape of the particle spectrum were unchanged by filtering.

B. Target Background

The Li isotopes were obtained from Oak Ridge National Laboratory. The Li^6 was of 99.3% isotopic purity. The maximum $\text{Li}^7(\gamma,t)$ cross section is about 0.2 mb.¹⁹ This is smaller than the $\text{Li}^6(\gamma,t)$ cross section measured by us. Since there was not more than 0.7% Li^7 in the target, the Li^7 contribution to the phototritons was negligible.

A possible source of prompt-background tritons is the (γ,n) reaction in the target. Since the target thickness was only about 5 μ , capture in the target of photo-neutrons would produce a negligible number of tritons.

By evaporating the Li in vacuum and maintaining it in vacuum at all times it was possible to eliminate the impurities which are most common, namely, the mineral oil used to preserve Li in storage, and nitride and hydride coatings which form with extreme rapidity in

air. The contribution of the Formvar backing to the photoparticle spectrum is small,⁶ and was subtracted.

C. Accelerator Background

Measures were taken to minimize the various sources of background which can be serious near pulsed electron beams of hundreds of milliamperes. The quadrupole triplet magnet was very important in this regard. By maintaining the detection solid angle for magnetically rigid, positively charged particles at a magnitude equivalent to a distance of a few inches between detector and target, while allowing the actual distance to be several feet, a reduction factor of over 100 was obtained for acceptance of photoelectrons, Compton electrons and photons, electron-positron pairs, scattered photons, rf power, etc., coming from the target and scattering chamber. The center stop of the magnet obscured the detector from direct view of the target. Various shielding materials were positioned as shown in Fig. 1.

When comparison runs were being made with various foil targets, it was found that pulse pileup increased markedly for Ni, and increased dramatically for Al (6- μ sheet). It disappeared when the target was raised out of the beam. This effect was present even when the electron gun of the accelerator was turned off, but the accelerating structure was being supplied with rf power. It was concluded that this pileup was due to rf radiation reflected from the target.

D. Unwanted Particles

The momentum-filtering capability of the magnet was of great value not only in eliminating electron and positron background but also in sorting the various charged-particle species and limiting the accepted energies of the interesting particles to correspond with the thickness of the detector. Otherwise "folding back" of the energy spectrum occurs as particles of ranges greater than the depletion-layer thickness traverse the detector. An apparent solution is to use thicker detectors. Horowitz and Sherman,^{20,21} for example, have used Li-drifted Si detectors 42 mm long, and Ge detectors 27 mm long, to study inelastic scattering of 100-MeV protons. However, in the photonuclear application, background is more severe. It increases with the depletion volume, so that the low-energy portion of the spectrum, perhaps several megavolts, lies buried in noise when the solid-state detector is thick enough to stop 30-MeV protons.

IV. RESULTS

The data described earlier⁶ came from spectra such as are shown in Fig. 3 which compare the photoparticles

¹⁸ D. J. Hughes and J. A. Harvey, in *Brookhaven National Laboratory Report No. 325* (U. S. Government Printing Office, Washington, D. C., 1955), pp. 65, 67.

¹⁹ M. Miwa and M. Yamanouchi, *J. Phys. Soc. Japan* **15**, 947 (1960).

²⁰ Y. S. Horowitz and N. K. Sherman, *Bull. Am. Phys. Soc.* **12**, 632 (1967).

²¹ Y. S. Horowitz and N. K. Sherman, *Can. J. Phys.* **45**, 3265 (1967), and references therein.

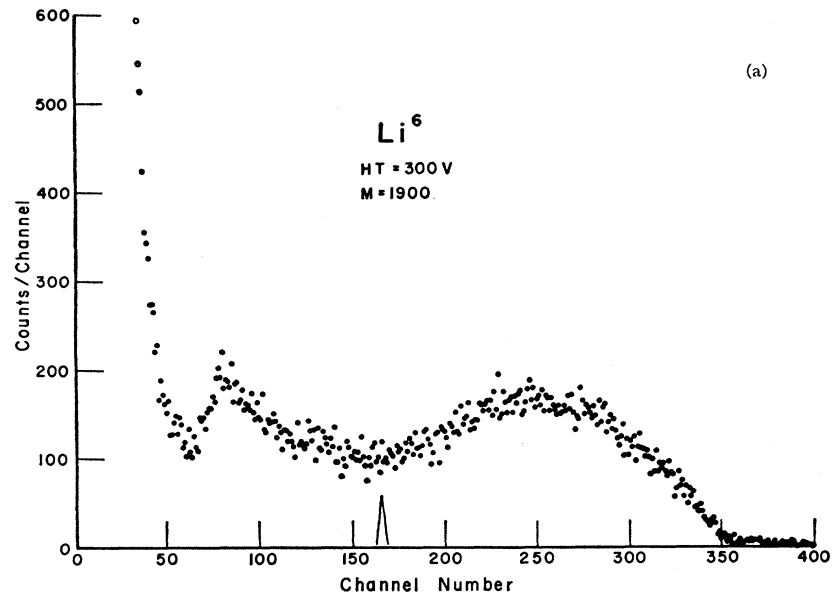
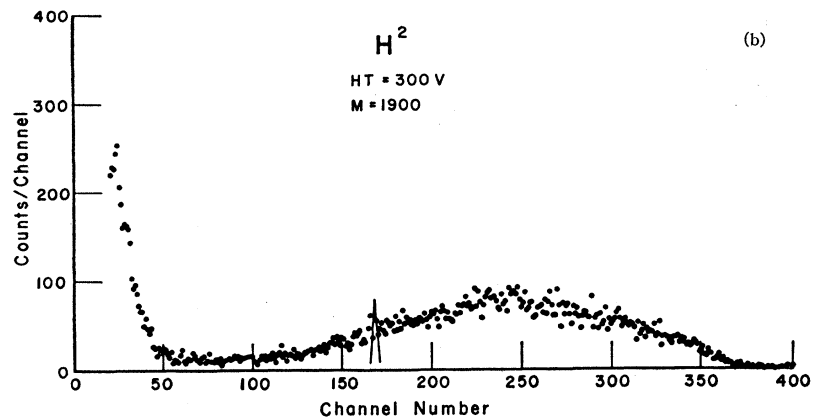


FIG. 3. (a) Thick detector spectrum of Li^6 , in which channel number is proportional to energy, which shows both a triton and a proton transmission peak. The peaks move up in energy as the magnet current (proportional to M) increases. (b) Thick detector spectrum of H^2 .



from Li with those from deuterium. These spectra were obtained with a thick detector depletion layer. Because the magnet focuses particles with large charge q and small momentum p most strongly, the ratio p/q determines the energy at which a given particle species will show a transmission maximum for a given magnet current setting. For example, protons and α particles are focused identically. One therefore expects at the transmission maximum,

$$T_p = 2T_d = 3T_t \quad (4)$$

and

$$\Gamma_p = 2\Gamma_d = 3\Gamma_t, \quad (5)$$

where T is the kinetic energy and Γ is the energy width of the transmission peak.

Figure 3(b) shows that the deuterium spectrum contains only photoprotons, as expected, while Fig. 3(a) shows that the Li spectrum contains tritons and protons,

but no appreciable number of deuterons. In fact, if the spectrum is interpreted as containing no deuterons, the triton cross section obtained by subtracting away the low-energy tail of the protons fits smoothly onto the data obtained with the thin depletion layer, where no tails need to be subtracted.

Figure 4 shows typical spectra obtained when the detector depletion layer is too thin to stop protons but thick enough to stop tritons. The large peak just above noise is the dE/dx peak for protons passing through the junction. The proton cutoff is evident in the deuterium case. Beyond this energy, the Li spectrum contains only tritons, with negligible background. Deuterons, if any, would lie higher in energy. It is spectra such as this which provided the new data, which appear as solid circles in Fig. 5.

No attempt was made to use the thin-detector tritons which overlaid the tip of the photoprotons near cutoff.

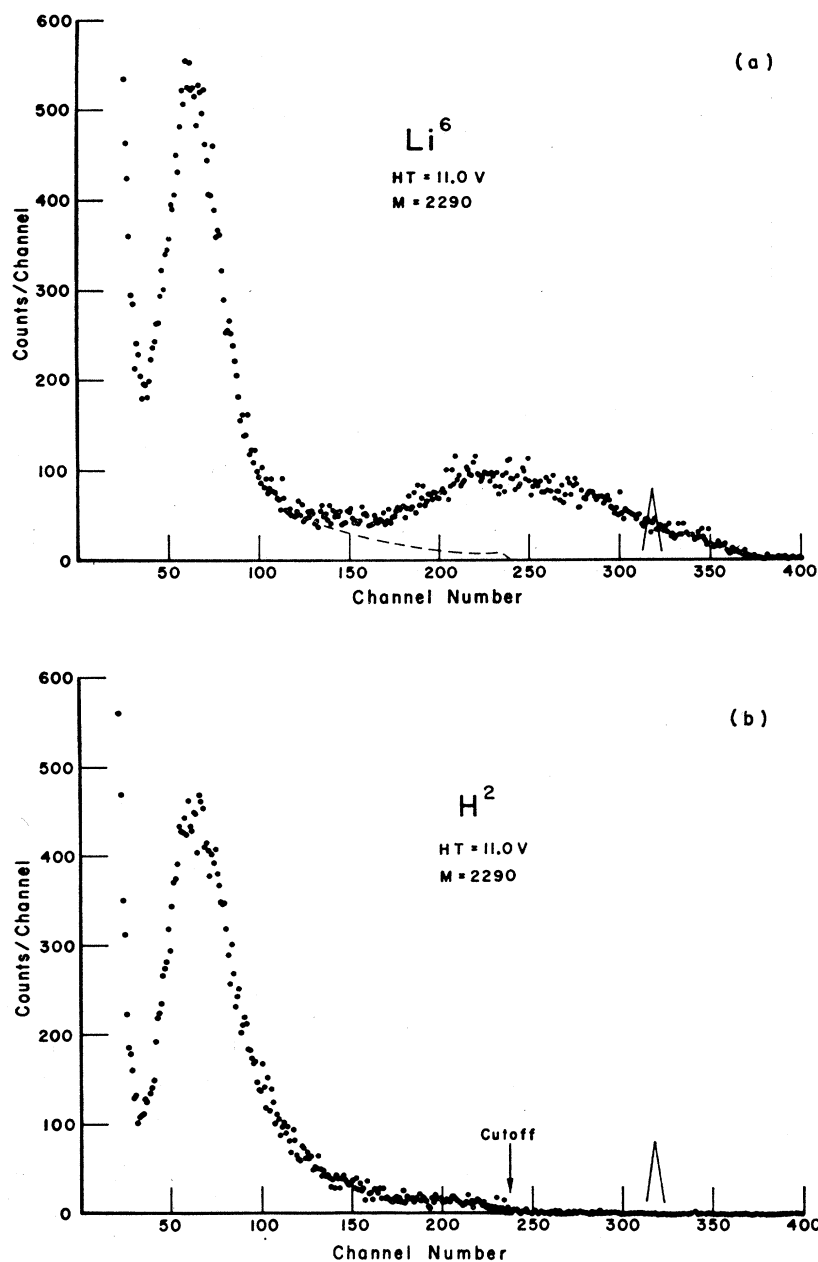


Fig. 4. (a) Triton spectrum of Li^6 obtained with thin depletion layer. The tall peak is due to protons passing right through the layer. Amplifier gain was about twice that of Fig. 3. (b) Thin detector spectrum of H^2 .

A simple subtraction of the tip shape obtained for deuterium is not sufficient, since the transmission function is slightly different depending on whether a solid or a gaseous target is used, and the photoproton cross sections of deuterium and Li^6 are not identical. In principle, however, the tip shape could have been calculated since both the transmission function and the photoproton yield were obtained during the experiment.

No correction was made for counting losses, which were less than 10% for Li. Their effect on the cross section was slightly overcompensated for by the deu-

terium counting losses, so that the cross section might be lowered a few percent by their inclusion.

Both peaks in Fig. 3(a) and the triton peak of Fig. 4(a) owe their shape mainly to the transmission function, because in the case of Li^6 the photoparticle cross sections vary slowly with energy when observed with 300-keV resolution. A target such as neon, which exhibits in its photoproton spectrum considerable level structure spaced about 1-MeV apart, may on the other hand have many peaks superimposed on a single transmission maximum.

In determining the total (γ, t) cross section absolutely, the $\text{H}^2(\gamma, p)$ -reaction cross section²² was taken as standard. Since only one angular position, namely, 90° , was measured, it was necessary to integrate over all angles to obtain the total cross section. It was assumed that the photoparticle angular distributions were the same in both reactions.

To obtain the cross section at 90° as a function of photon energy the transmission function must be unfolded from the experimental maxima. The transmission function corresponding to a foil target was obtained by observing the change in counting rate in particular Li photoproton energy channels while only the magnet current setting was varied. The resulting measured function is shown in Fig. 2. The reduced coordinate P^2 corresponds to energy divided by the square of the magnet current.

The cross-section curve obtained from the data is shown in Fig. 5. Above 19 MeV, the solid line is an average of the experimental points. Below 19 MeV, it is a free-hand extrapolation with the constraints that the threshold for the (γ, t) reaction is 15.791 MeV²³ and that the cross section at 17.6 MeV is very small.¹ Errors are estimated in Appendix C.

V. DISCUSSION

We ascribe the observed phototriton yield to electric-dipole absorption. Isospin selection rules do not allow the reactions $\text{Li}(\gamma, d)\text{He}^4$ and $\text{Li}^6(\gamma, 2d)\text{H}^2$ to result from $E1$ or $M1$ photon absorption.^{24,25} These reactions are allowed, however, for $E2$ radiation. Deuterons can also be produced by $E1$ transitions through 3-body decay into $\text{H}^1 + \text{H}^2 + \text{H}^3$ or $n + \text{H}^2 + \text{He}^3$. The deuteron yield, then, sets a conservative upper limit on the amount of $E2$ absorption occurring. The strengths of $E2$ and $M1$ transitions are expected to be comparable, and much weaker than $E1$. Experiment shows that 2-body deuteron yield is negligible.

Using dispersion relations, Gell-Mann, Goldberger, and Thirring⁷ deduced the following sum rule for nuclear photodisintegration by $E1$ transitions:

$$\sigma_{\text{int}} = 0.060(NZ/A)(1 + 0.1A^2/NZ), \quad (6)$$

where

$$\sigma_{\text{int}} = \int_0^\mu \sigma_k dk \quad (7)$$

is the integrated cross section in MeV b, μ is the threshold energy for meson photoproduction, and σ_k is the total photonuclear cross section for photons of energy

²² J. J. de Swart and R. E. Marshak, *Physica* **25**, 1001 (1959).

²³ F. Everling, L. A. Koenig, J. H. E. Mattauch, and A. H. Wapstra, in *1960 Nuclear Data Tables*, compiled by K. Way *et al.* (Printing and Publishing Office, National Academy of Sciences—National Research Council, Washington 25, D. C., 1961), Part 1, p. 10.

²⁴ L. E. H. Trainor, *Phys. Rev.* **85**, 962 (1952).

²⁵ G. Morpurgo, *Phys. Rev.* **110**, 721 (1958).

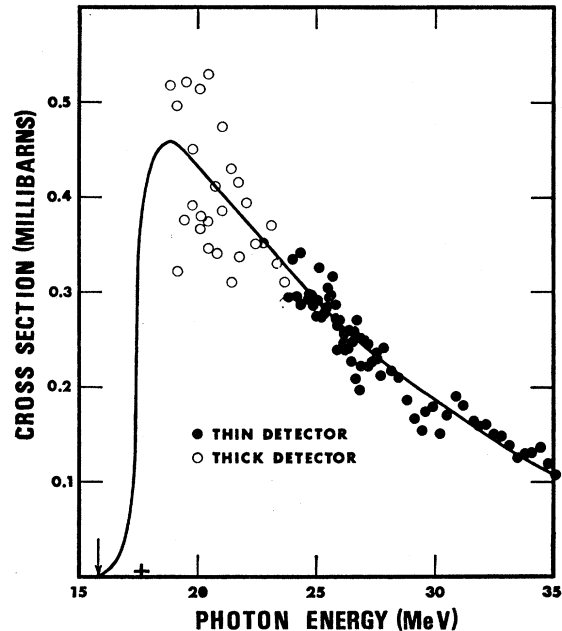


FIG. 5. Phototriton cross section of Li^6 . The arrow indicates the reaction threshold. The cross represents the result of Ref. 1, the open circles that of Ref. 6, the solid circles that of the present work. The solid line, above 19 MeV, is an average of the experimental points.

k . For Li^6 , the predicted σ_{int} is 126 MeV mb. If the term proportional to A in Eq. (6) were neglected, σ_{int} would be 90 MeV mb. For the partial cross section $\sigma(\gamma, t)$ we find experimentally that

$$\int_{19}^{35} \sigma(\gamma, t) dk = 4.9 \pm 2.5 \text{ MeV mb.}$$

We can add this to the $\sigma(\gamma, n2p)$ and $\sigma(\gamma, pd)$ obtained by Denisov *et al.*,¹¹ who obtained 5 MeV mb as the integrated cross section between 36 and 55 MeV, to obtain an experimental value of about 10 MeV mb for the integrated phototriton cross section up to 55 MeV. Adding $\sigma_{\text{int}}(t)$ to the σ_{int} for all other processes obtained by Denisov *et al.* gives 70 ± 20 MeV mb as the total integrated cross section of Li^6 .

The so-called “bremsstrahlung-weighted cross section,”

$$\sigma_b \equiv \int_0^\infty \frac{\sigma}{k} dk, \quad (8)$$

is related to the mean-square nuclear-charge radius $\langle r_c^2 \rangle$ and the mean-square proton radius $\langle r_p^2 \rangle$ by the equation²⁶⁻²⁹

$$\sigma_b(E1) = (4\pi^2\alpha ZN/3A^*) (\langle r_c^2 \rangle - \langle r_p^2 \rangle), \quad (9)$$

²⁶ J. S. Levinger and H. A. Bethe, *Phys. Rev.* **78**, 115 (1950).

²⁷ L. L. Foldy, *Phys. Rev.* **107**, 1303 (1957).

²⁸ Yu. K. Khokhlov, *Dokl. Akad. Nauk* **97**, 239 (1954).

²⁹ J. S. Levinger and D. C. Kent, *Phys. Rev.* **95**, 418 (1954).

where $\alpha = e^2/\hbar c$ is the fine-structure constant and $A^* = (A-1)/(1-\Lambda)$ in the Khokhlov²⁸ formulation, with $\Lambda = 0.84/(1+22/A)$. For phototritons between 19 and 35 MeV, we have obtained experimentally $\sigma_b(t) = 0.18 \pm 0.09$ mb. For photoneutrons between 5.55 and 32.05 MeV, the Livermore group obtained $\sigma_b(n) = 1.85 \pm 0.10$ mb. Denisov *et al.* obtained 3.7 ± 0.4 mb for all processes up to 55 MeV. The present results indicate that their figure should be reduced to 3.4 ± 0.4 mb. This corresponds to a nuclear charge radius of 1.75 ± 0.1 F. The rms radius obtained from a phenomenological fit to electron scattering³⁰ is 2.54 ± 0.05 F. This value can be reduced to 2.31 F by suitable choice of nuclear wave function.³¹

Foldy proposed²⁷ that Li^6 might have a structure consisting of an α particle and two loosely bound nucleons. If this is so, then the bremsstrahlung-weighted cross section can be written as

$$\sigma_b(\text{Li}^6) = \sigma_b(\text{He}^4) + \left(\frac{1}{3}\pi^2\alpha\right)\langle r^2 \rangle, \quad (10)$$

where $\langle r^2 \rangle$ is the mean-square separation of the two orbital nucleons. Furthermore, the rms charge radius of Li^6 obeys the relation

$$\langle r_c^2 \rangle = 2/9\langle \rho^2 \rangle + \frac{1}{12}\langle r^2 \rangle + \frac{2}{3}\langle r_\alpha^2 \rangle + \frac{1}{3}\langle r_p^2 \rangle, \quad (11)$$

where $\langle \rho^2 \rangle$ is the mean-square separation of the c.m. of the α particle and the c.m. of the two orbital nucleons, and $\langle r_\alpha^2 \rangle$ is the mean-square charge radius of He^4 . Using the values $\sigma_b(\text{He}^4) = 2.40$ mb,³² $\langle r_p^2 \rangle^{1/2} = 0.805$ F,³³ $\langle r_\alpha^2 \rangle^{1/2} = 1.71$ F,³⁴ and $\langle r_c^2 \rangle^{1/2} = 2.31$ F³¹ in Eqs. (10) and (11), we find that $\langle r^2 \rangle^{1/2}$ is 2.0 F and $\langle \rho^2 \rangle^{1/2}$ is 1.6 F.

It has been pointed out by G. M. Temmer³⁵ that the reaction $\text{Li}^6(\gamma, \text{H}^3)\text{He}^3$ can be used to test charge independence of the nuclear force. This requires the performance of a careful angular distribution experiment.

ACKNOWLEDGMENTS

We wish to thank the laboratory staff for technical assistance and Professor H. L. Schultz for his hospitality. Support from the National Research Council of Canada to N. K. S. is also gratefully acknowledged.

APPENDIX A. CALCULATION OF PHOTON ENERGY

If the particle emitted backward in the c.m. of a 2-body equal-mass final state is detected at 90° to the incident photon beam, a simple relation exists between

³⁰ L. R. Suelzle, M. R. Yearian, and H. Crannell, *Phys. Rev.* **162**, 992 (1967).

³¹ D. L. Lin and S. S. M. Wong, University of Rochester Report No. UR-875-176, 1966 (unpublished).

³² A. N. Gorbunov, V. A. Dubrovina, V. A. Osipova, V. S. Silaeva, and P. A. Cerenkov, *Zh. Eksperim. i Teor. Fiz.* **42**, 747 (1962) [English transl.: *Soviet Phys.*—*JETP* **15**, 520 (1962)].

³³ L. N. Hand, D. G. Miller, and R. Wilson, *Rev. Mod. Phys.* **35**, 335 (1963).

³⁴ R. F. Frosch, J. S. McCarthy, R. E. Rand, and M. R. Yearian, *Phys. Rev.* **160**, 874 (1967).

³⁵ G. M. Temmer (private communication).

the laboratory and c.m. energies. Neglecting the difference in mass between the excited nucleus and its ground state,

$$k = 2T + T_0 + Q, \quad (A1)$$

where T is the particle energy in the c.m. frame. The recoil energy T_0 of the target nucleus arising from the photon momentum is

$$T_0 = p_0^2/2M, \quad (A2)$$

where

$$p_0 = k/\sqrt{\mu} \quad (A3)$$

is the photon momentum, M is the mass of the nucleus in atomic mass units, and the constant μ has the value 931.478 MeV/amu. For binary breakup into fragments of equal mass m , the laboratory kinetic energy is

$$T_i = T + \frac{1}{2}T_0 + \delta T_i, \quad (A4)$$

where

$$\delta T_i = (p_T p_0/2m) \cos \theta_i, \quad i=1, 2 \quad (A5)$$

and θ_i is the emission angle in the c.m. of the i th particle measured from the beam direction. In units of $\text{amu}^{1/2}$ MeV^{1/2},

$$p_T = (2mT)^{1/2}. \quad (A6)$$

In this experiment if a triton is forward-going in the c.m., it will fall outside the magnet acceptance. For 20-MeV photons on Li^6 a triton emitted at 90° in the c.m. is shifted forward by 5.3° in the laboratory, compared to the magnet acceptance half-angle ϕ of 3° in the horizontal (initially defocusing) plane. At 30 MeV, the angle shift is 4.3° , still greater than ϕ . The detected particle will therefore always correspond to subscript 1, denoting backward-going. For the case of emission of fragment 1 at 90° in the laboratory,

$$\theta_1 = \frac{1}{2}\pi + x, \quad (A7)$$

so that

$$\cos \theta = -\sin x = -p_0/p_T. \quad (A8)$$

Hence

$$\delta T_1 = -p_0^2/2M = -T_0. \quad (A9)$$

We find that

$$T_1 = T - \frac{1}{2}T_0 \quad (A10)$$

and

$$T_2 = T + \frac{3}{2}T_0.$$

Therefore,

$$k = 2T_1 + k^2/M\mu + Q. \quad (A11)$$

If in the case of Li^6 we choose, for example, $k = \sqrt{\mu}$ = 30.5 MeV, then $T_1 = 7.3$ MeV and the quadratic recoil term in Eq. (13) has a value of 167 keV.

Recoil causes the excitation energy E^* of the target to differ slightly from the photon energy:

$$E^* = k - T_0 = 2T_1 + Q + T_0. \quad (A12)$$

In the case just mentioned, T_0 is 83 keV.

The correction to the photon energy due to the average energy loss of 2-MeV tritons originating at any depth in the target was about 100 keV and was less for higher-energy tritons.

APPENDIX B. ENERGY RESOLUTION

There are three main sources of uncertainty in the photon energy calculated from the measured triton energy. First, there is the possibility of 3-body breakup, which we neglect because of the small number of deuterons observed. Denisov *et al.*¹¹ confirm this below 40 MeV. Second, there is the finite detector resolution. If the detector resolution Γ is independent of triton energy,

$$k \simeq 2(T_1 \pm \Gamma) + Q, \quad (\text{B1})$$

so that $(\Delta k)_\Gamma = \pm 2\Gamma$, or about 260 keV in this case. Third, there is the finite angular acceptance of the quadrupole magnet. Equation (A4) shows that due to recoil the laboratory kinetic energies of the photo-particles depend upon the detection angle. The azimuthal acceptance half-angle ϕ of about 3° introduces an uncertainty of about 80 keV at 20 MeV, and about 230 keV at 30 MeV. The photon-energy spread $(\Delta k)_\phi$ corresponding to a detected energy T_1 can be obtained from the difference between the values of k calculated for the limiting values of θ_1 which correspond to emission angles of $\frac{1}{2}\pi \pm \phi$. If we denote the difference between the laboratory emission angle θ_L and the c.m. angle θ by ψ ,

$$\theta = \theta_L + \psi, \quad (\text{B2})$$

then the limiting values of θ_1 are

$$\theta_1' = \frac{1}{2}\pi + \phi + \psi'$$

and

$$\theta_1'' = \frac{1}{2}\pi - \phi + \psi''. \quad (\text{B3})$$

Since ψ is a small angle,

$$\psi' \simeq p_0/2p_{T1} \simeq \psi''. \quad (\text{B4})$$

Now from Eq. (A1) and (A4)

$$(\Delta k)_\phi \equiv k' - k'' = (p_{T1}'' p_0''/m) \cos\theta_1'' - (p_{T1}' p_0'/m) \cos\theta_1'. \quad (\text{B5})$$

Making the approximation

$$p_{T1}'' p_0'' \simeq p_{T1} p_0 \simeq p_{T1}' p_0', \quad (\text{B6})$$

where the unprimed quantities refer to the central ray,

$$(\Delta k)_\phi \simeq 2\phi k (2T_1/m\mu)^{1/2}. \quad (\text{B7})$$

If we combine $(\Delta k)_\Gamma$ and $(\Delta k)_\phi$ quadratically, we find the over-all experimental resolution to be 332 keV at 30 MeV and 272 keV at 20 MeV.

Emission of a particle out of the horizontal plane leads to somewhat larger limiting values of θ , and hence larger values of δT . However, in this case the correction is negligible.

APPENDIX C. ERROR IN CROSS SECTION

In obtaining the Li⁶ cross section relative to deuterium, it was necessary to know the thickness of each element exposed to the photon beam. The deuterium gas pressure was measured to an accuracy of better than 1%. The effective length of the gas target was defined by the magnet acceptance.³⁶ A value of 0.68 \pm 0.06 in. was used. The thickness of Li in the target was measured by obtaining the unshifted α -particle energy, the energy shifted by the Formvar, and the energy shifted by Formvar plus Li. From the range-energy relation³⁷ the Li thickness was found to be 0.22 \pm 0.04 mg/cm².

The absolute deuterium cross section as a function of photon energy²² is probably not known to better than 10%. Systematic error arising from the transmission function is about 3%. A further source of error was the bremsstrahlung spectral shape, which contributed about 9%.

We conclude that systematic error in the magnitude of the cross section shown in Fig. 5 can be about 52%. That the order of magnitude of the cross section is correct is indicated by the fact that the Li⁶(γ, p) cross section, calculated with the same errors, agrees⁶ within error with the (γ, p) cross section deduced from the Livermore measurements.⁵

³⁶ J. R. Stewart (private communication).

³⁷ W. Whaling, in *Handbuch der Physik*, edited by S. Flugge (Springer-Verlag, Berlin, 1958), Vol. 34, p. 193.